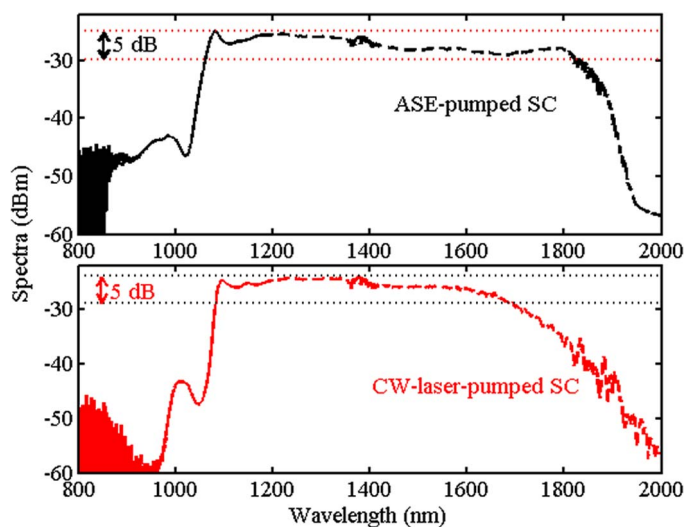


High-Power Ultraflat Near-Infrared Supercontinuum Generation Pumped by a Continuous Amplified Spontaneous Emission Source

Volume 7, Number 2, April 2015

Aijun Jin
Hang Zhou
Xuanfeng Zhou
Jing Hou
Zongfu Jiang



DOI: 10.1109/JPHOT.2015.2416122
1943-0655 © 2015 IEEE

High-Power Ultraflat Near-Infrared Supercontinuum Generation Pumped by a Continuous Amplified Spontaneous Emission Source

Aijun Jin, Hang Zhou, Xuanfeng Zhou, Jing Hou, and Zongfu Jiang

College of Optoelectronic Science and Engineering, National University of Defense Technology, Changsha 410073, China

DOI: 10.1109/JPHOT.2015.2416122

1943-0655 © 2015 IEEE. Translations and content mining are permitted for academic research only. Personal use is also permitted, but republication/redistribution requires IEEE permission. See http://www.ieee.org/publications_standards/publications/rights/index.html for more information.

Manuscript received March 4, 2015; revised March 19, 2015; accepted March 19, 2015. Date of publication March 24, 2015; date of current version April 1, 2015. This work was supported in part by the State Key Program of the National Natural Science Foundation of China under Grant 61235008, by the Hunan Provincial Natural Science Foundation of China under Grant 14JJ3001, and by the Postgraduate Innovation Foundation of the National University of Defense Technology, China, under Grant B140704. Corresponding author: A. Jin (email: jin_ajun@163.com).

Abstract: A high-power ultraflat near-infrared supercontinuum (SC) is generated in a section of photonic crystal fiber (PCF) pumped by an amplified spontaneous emission (ASE) source instead of continuous-wave (CW) and pulsed lasers. A low-power ASE seed at 1 μm is amplified to be 90.9 W by two fiber amplifiers and then emitted from a 10- μm -core fiber. Using this ASE source to pump a section of 100-m-long PCF, a 49.5-W near-infrared SC is obtained, and the 5-dB spectral bandwidth is 760 nm, covering from 1062 to 1822 nm. This is the reported highest power of ASE-pumped SC source. A comparative experiment is taken with a 122-W CW laser at 1090 nm to pump the same PCF. A 56.2-W SC source is generated with 5-dB spectral width of 605 nm from 1082 to 1687 nm. The conversion efficiency to SC is higher, and the spectrum is broader and flatter using the ASE source as the pump. Conclusively, pump incoherence can aid the SC generation and spectral flatness.

Index Terms: Supercontinuum generation, amplified spontaneous emission.

1. Introduction

A supercontinuum (SC) source generated in optical fiber is attractive for many fields such as optical coherence tomography, optical frequency metrology, and optical communications and has experienced rapid development in the past decade based on well-known underlying mechanisms [1]–[3]. The most common configuration of SC generation is pumping a section of photonic crystal fiber (PCF) by pulsed laser from femtosecond to nanosecond regime [4], [5]. Another common pump source is continuous-wave (CW) laser. The CW-laser-pumped SC presents significant advantages over pulsed-laser-pumped SC including higher spectral power densities and smoother spectra [6]–[13]. As reported in many papers, pump incoherence can aid the spectral broadening and smoothing of CW-laser-pumped SC [14]–[19] through seeding the break-up of pump light by modulation instability (MI). As a low-coherence CW light, amplified spontaneous emission (ASE) has been used to be the pump source for SC generation

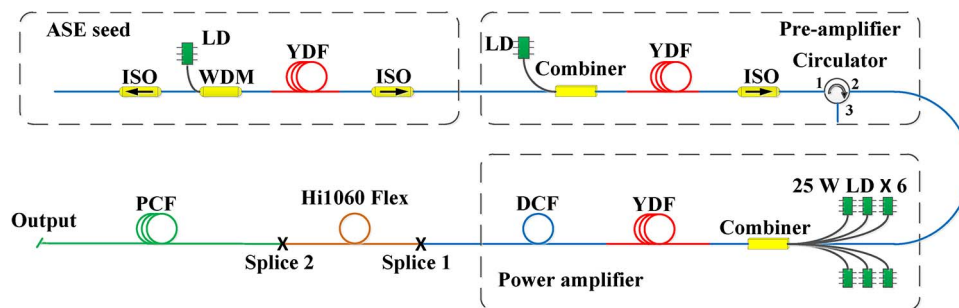


Fig. 1. Schematic diagram of the configuration of ASE-pumped SC generation. LD: laser diode. WDM: wavelength division multiplexer. YDF: Yb-doped fiber. ISO: isolator. Splice 1 and Splice 2 are the splice points of the DCF and Hi1060 Flex and the Hi1060 Flex and PCF, respectively.

[20]–[22]. Generally, ASE sources used to be as the pump to generate SCs can be divided into two classes: Er-based ASE and Yb-based ASE.

When using CW source to pump SC generation, the pump sources should locate in the anomalous dispersion region of nonlinear fiber. Thus, the MI effect can aid the split of the pump source into short pulses and induce SC generation. Normally commercial Si-fibers have their zero-dispersion wavelengths (ZDW) longer than 1300 nm. This makes Er-based ASE a good pump source for SC generation [16], [20]–[25]. As we have known, the highest power of ASE source emitted from Er or Er/Yb doped fiber is commonly tens of watts [26], [27]. The reported ASE-pumped SCs are all as low as some watts. In order to satisfy the excitation requirements of nonlinear effects, two methods are adopted which are using ultra-long nonlinear fibers [16], [20]–[24] and modulating the ASE source into noise bursts [25]. These two methods both make the structure more complex. And the most importantly, Er-based ASE and Er-ASE-pumped SC cannot reach high output power.

Yb-based ASE is located around 1 μm which is in the normal dispersion region of ordinary Si-fibers and distant from the ZDW. In the reports of Yb-based ASE-pumped SCs [28], [29] PCF which has a ZDW of 1040 nm is used as the nonlinear fiber. Additionally, the ASE sources are also modulated into noise bursts and thus the advantages of CW-pumped SC vanish. The highest power of Yb-based ASE source is around a hundred watts [30]–[32]. However, the fibers used for high-power ASE all have large cores around 20 μm , which introduces a large mode-field mismatch with the nonlinear fiber. Thus the power of ASE source used for SC generation is limited and the power of SC is very low. The spectral range and spectral flatness of the generated SC source are also influenced by the low power.

In this paper, we report a high power ultra-flat near-infrared SC source pumped by an ASE source from Yb-doped fiber (YDF). A 90.9 W ASE source around 1 μm is obtained based on a two-stage fiber amplifier configuration with a low power ASE seed. The output fiber of the ASE source has a core of 10 μm , which is close to that of the PCF used as the nonlinear medium for SC generation. The ASE source is coupled into the PCF to generate a 49.5 W SC with a 5-dB spectral bandwidth of 760 nm covering from 1062 nm to 1822 nm. In addition, a comparative experiment is taken using a 122 W CW laser at 1090 nm as the pump light.

2. Experimental Setup

The experimental setup of ASE-pumped SC generation is schematically shown in Fig. 1. The whole structure comprises four parts: an ASE seed, a pre-amplifier, a power amplifier, and the SC-generation PCF.

The ASE seed is constructed in a single-pass forward pumping configuration. A piece of 50 cm long single-mode YDF with a 4 μm core is used as the active medium for the ASE source generation. The core numerical aperture (NA) is 0.2, and the peak core absorption at 976 nm is about 1200 dB/m. A 565-mW laser diode (LD) at 976 nm is coupled into the gain fiber through a wavelength division multiplexer (WDM) as the pump light. At the two ends of the ASE seed structure,

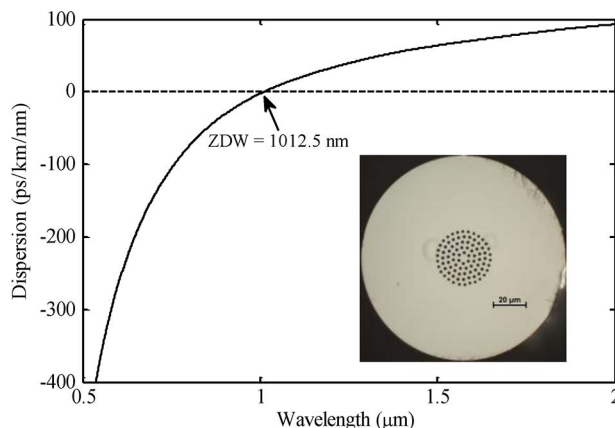


Fig. 2. Calculated dispersion of the used PCF. The inset shows the cross section.

the signal port of the WDM and the output end of the gain fiber, two isolators are spliced to prevent the reflectivity from the fiber end and suppress lasing at a high pump power level.

The output ASE seed is coupled into a section of YDF as the signal light of a fiber amplifier through a $(2 + 1) \times 1$ signal-pump fiber combiner. The gain fiber is a 4.5 m Yb-doped double-clad fiber (DCF) with a cladding absorption of 3.9 dB/m at 976 nm. The gain fiber is forwardly pumped by a fiber-pigtailed multimode LD at 976 nm. The core of the gain fiber has a diameter of 10 μm and a NA of 0.075, and its inner cladding has a diameter of 130 μm and a NA of 0.46. The output fiber of the pump LD has a core of 105 μm , and the maximum output power is 9 W. A high power isolator with 32 dB isolation covering 100 nm centered at 1064 nm is spliced to the output end of the gain fiber. A high-power circulator is connected to the isolator. The isolator and circulator are used to prevent reflected light into the gain fiber.

In the power amplifier, a section of 8 m long YDF with core/inner-clad diameter of 10/125 μm is used as the gain medium. The NA of core and inner clad are 0.08 and 0.46 respectively. Its cladding absorption is 6.9 dB/m at 976 nm. The ASE signal from the pre-amplifier is amplified with 6 fiber-pigtailed LDs with maximum 25 W output power for each one and the pigtail fiber has a core of 105 μm . The signal light and pump lights are combined into the gain fiber through a $(6 + 1) \times 1$ signal-pump fiber combiner. A section of 1-m-long passive DCF is used as the output fiber.

A piece of 100 m long PCF is utilized as the nonlinear fiber for ASE-pumped SC generation. This kind of PCF is composed of five rings of circular air-holes with a hole diameter of 2.05 μm and a pitch of 3.35 μm as shown in the inset of Fig. 2. The calculated dispersion of the PCF is depicted in Fig. 2 demonstrating that the ZDW is 1012.5 nm. The effective mode area at 1090 nm is 11.5 μm^2 and the corresponding nonlinear coefficient is 60 ($\text{W} \cdot \text{km}^{-1}$). Due to the large mode area mismatch between the PCF and the output fiber of the ASE source, a direct splice will bring high loss. Thus a section of Hi1060 Flex fiber (mode field diameter 4 μm at 980 nm) manufactured by Corning Incorporated is used as a bridge fiber. One end of this fiber is thermally expanded in its core to match the mode field of the output fiber of the ASE source [33]. The other end is spliced with the PCF directly due to the matched mode fields. The output facet of the PCF is angle-cleaved at 9° to avoid Fresnel reflection.

3. Results and Discussion

3.1. High-Power ASE Source

The ASE seed power is 39.3 mW with the highest pump power 565 mW and the spectrum is shown in Fig. 3(a). The highest peak of the spectrum is located around 1030 nm. The spectrum is cut abruptly around 980 nm because of the absorption of the gain fiber at about 976 nm. In

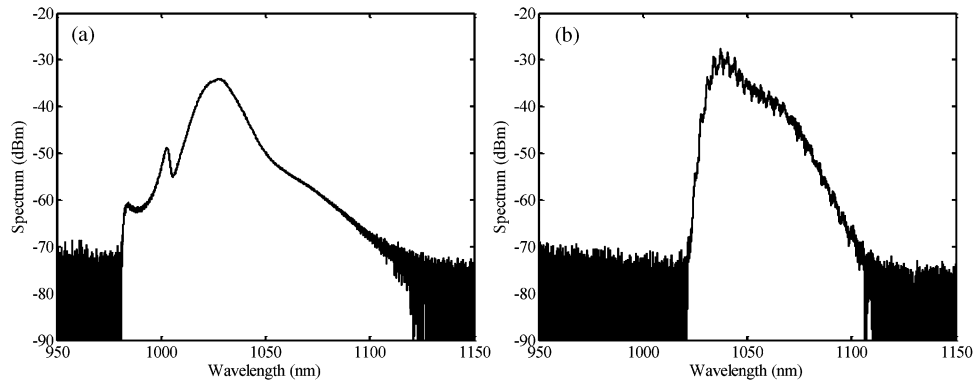


Fig. 3. (a) Spectrum of the ASE seed with 39.3 mW output power. (b) Spectrum of the ASE with 2.47 W power output from the pre-amplifier.

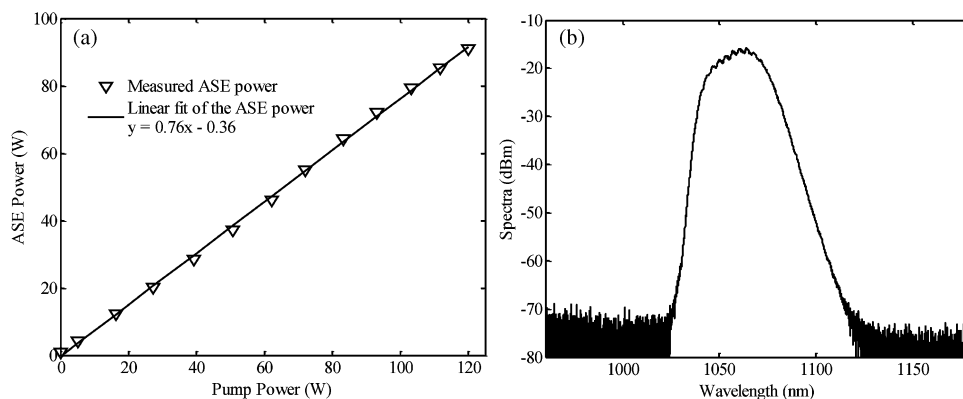


Fig. 4. (a) Amplified ASE power versus pump power in the power amplifier. (b) Spectrum of ASE light with 90.9 W output power.

addition, there is a slight peak at 1000 nm, which may be induced by the special gain characteristic of the active fiber.

The ASE seed as a signal light is coupled into the pre-amplifier. When the pump power is 5.8 W the output ASE light is 2.47 W and the spectrum is shown in Fig. 3(b). The peak is shifted to 1040 nm. From the figure we can find some ripples in the spectrum. This is because the fiber core of the high-power circulator is 15 μm which is larger than the 10- μm -core fiber of the pre-amplifier; thus the splice of these two fibers excites higher order mode and inter-mode interference.

In the power amplifier the ASE light is amplified to 90.9 W and the power characteristic is shown in Fig. 4(a). The pump powers are measured at the output of combiner and the maximum value is 120 W. The ASE power is augmented linearly with the pump power and the slope efficiency is about 76%. From the figure it can be known that with higher pump power the ASE light can be amplified further. The spectrum of the ASE source with the maximum output power is shown in Fig. 4(b). The 3-dB bandwidth is 23 nm covering from 1049 nm to 1072 nm. To our best knowledge, this is the reported highest power of ASE source output from such a fiber with a core of 10 μm diameter. The advantage of adopting such a small-core fiber is decreasing the mode-field mismatch of the fiber and the PCF and simplifying the splice of these two fibers.

3.2. SC Generation Pumped by the ASE Source

The mode field area of the output fiber of the ASE source is 101.6 μm^2 at 1060 nm while that of the PCF used here for SC generation is 11.4 μm^2 . This large mode field mismatch makes a

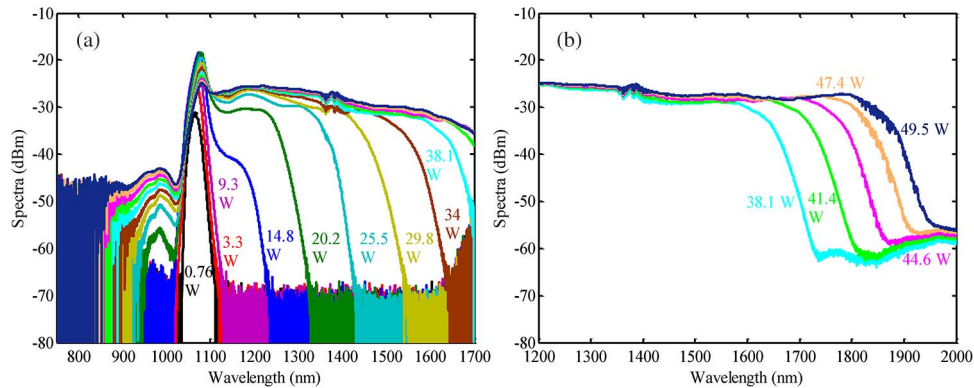


Fig. 5. Output spectra of generated SC pumped by ASE sources. The colored legend presents the power of corresponding spectrum marked by the same color. (a) Spectra below 1700 nm measured by OSA1. (b) Spectra measured by OSA2.

low-loss splice difficult, and thus, a bridge fiber is used. Here we adopt a short section of Hi1060 Flex fiber which core NA is 0.22 as the bridge fiber. The mode field area is $13.6 \mu\text{m}^2$ at 1060 nm and direct splice is taken between the bridge fiber and the PCF. The core of the other end of bridge fiber is thermally expanded to match the mode field area of the output fiber of the ASE source [33].

A piece of 100 m PCF is applied to generate SC using the obtained ASE source. The measured output spectra at different output powers are shown in Fig. 5(a) and (b). Spectra shorter than 1700 nm measured by an optical spectrum analyzer (OSA1, Yokogawa AQ6370C) are shown in Fig. 5(a), while the spectra longer than 1700 nm are measured by OSA2 (Yokogawa AQ6375) and shown in Fig. 5(b).

From Fig. 5(a) and (b) it can be found that when the output power is lower than 9.3 W no non-linear phenomena appear, but the peak of the output light shifts to longer wavelength due to the reabsorption of the gain fiber. As the output power reaches 14.8 W the spectrum is broadened to longer wavelength region evidently. Because the ZDW of PCF is 1012.5 nm, the ASE source locates in the anomalous dispersion region. Thus the spectral broadening is originated from MI which splits the CW ASE source into numerous fundamental solitons. Then due to soliton self-frequency shift (SSFS) effect the spectrum is shifted to longer wavelength region which can be seen in Fig. 5(a) when the output power is higher than 14.8 W. Additionally, because MI is seeded from noise, the formed solitons will have variable bandwidths and duration. For different solitons, the intra Raman scattering, e.g., SSFS, will induce different red-shift spectra. And a superposition of the numerous soliton red-shift spectra forms a smooth spectral extension [34]. This can be verified by Fig. 5(a) and (b).

The soliton frequency shift through a fiber can be given approximately by the following equation [34]:

$$\frac{\partial\omega}{\partial z} \propto P_{cw}^2$$

where z is the propagation distance, and P_{cw} is the average continuous pump power, which stands for the ASE power here. From the equation we can know that high ASE power can lead to a large spectral expansion. As seen in Fig. 5 with the increase of pump power, the generated SC spectrum is extended to longer wavelength. Pumped by the highest ASE power, the spectrum can be broadened to 1900 nm.

From Fig. 5(a) it also can be seen that a spectral component at a very low level emerges in the short wavelength region of the ASE source. When the power of ASE source is 28.4 W, the output power is 20.2 W and the short wavelength expansion is firstly observed which is located around 985 nm. This phenomenon can be interpreted by the excitation of dispersive waves. By

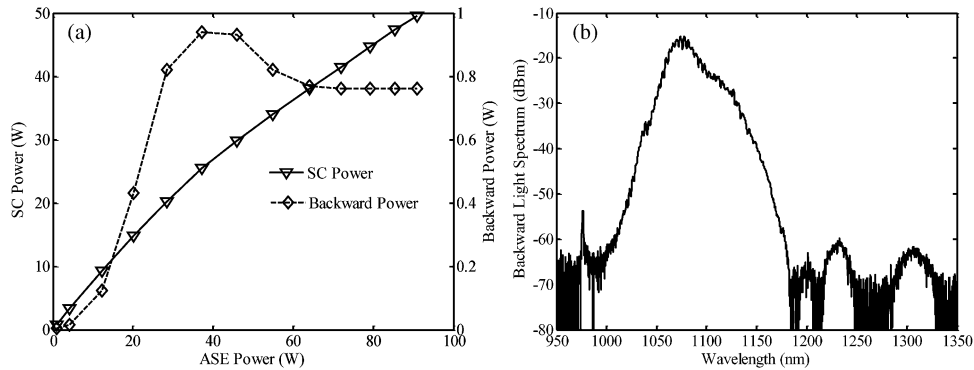


Fig. 6. (a) SC power and backward power versus ASE power. (b) Spectrum of the backward light when the ASE power is 90.9 W. The output power is 49.5 W.

increasing the ASE power, the dispersive waves are augmented and expand the spectrum to shorter wavelength as the figure shows.

The output power and backward power versus ASE power is shown in Fig. 6(a). The backward power is measured at the third port of the circulator. The slope efficiency of output power versus ASE power decreases slowly. This is because the loss resulted from quantum defect is increased when the spectrum is extended to longer wavelength with the enhancement of ASE power. When the ASE power is at the highest value 90.9 W the output SC power is 49.5 W.

However, the backward power rises first when the ASE power is lower than 37.3 W and then decreases with the increase of ASE power. The spectrum of the backward light at the highest SC output power is shown in Fig. 6(b). From the figure it can be known that the light output from the third port of the circulator covers a spectral range from 1000 nm to 1350 nm mainly which is related with the operating wavelength range of the circulator. This can be used to explain the change trend of the backward power versus ASE power. When the ASE power is lower than 37.3 W the output spectrum is shorter than 1400 nm, thus the backward power rises to its summit 0.94 W. Then increasing the ASE power further, the output spectrum is extended to longer wavelength region. The power of spectral components shorter than 1400 nm decreases, resulting in the decrease of backward power.

3.3. Comparative Experiment Using CW Laser to Pump the Same PCF to Generate SC

In order to compare the process of SC generation pumped by ASE source and CW laser, a CW laser at 1090 nm is adopted to pump the same PCF. The structure of the CW laser is the same as described in the reference [35]. Finally, the output power can reach 56.2 W with a 122 W CW laser.

The spectra at different power levels are shown in Fig. 7(a) and (b). The spectral evolution is similar to that of the ASE-pumped SC generation. However, from Fig. 7(a) and (b) it can be observed that the red-shift spectrum is not as flat as that of the ASE-pumped SC and the spectral extension range is smaller. This difference is resulted from the noise characteristic of pump source, which plays dominant role in seeding MI effect. Because ASE source has large phase and intensity fluctuations due to its incoherence, the solitons generated have random bandwidths and durations as mentioned in the former section. While the CW laser has better temporal coherence and the phase and intensity fluctuations are weaker. Consequently the ASE-pumped SC is more flat than the CW-laser-pumped SC. In addition the randomness of generated solitons due to temporal fluctuations can strengthen the soliton collisions, which is an important aid for the spectral red-shift further. Thus the ASE-pumped SC has a broader spectral range.

The spectra of two SCs pumped by 90.9 W ASE source and 122 W CW laser, respectively, are shown in Fig. 8. From the figure, it can be clearly seen that the ASE-pumped SC has broader and smoother spectrum. The CW-laser-pumped SC is 56.2 W with 5-dB spectral width 605 nm

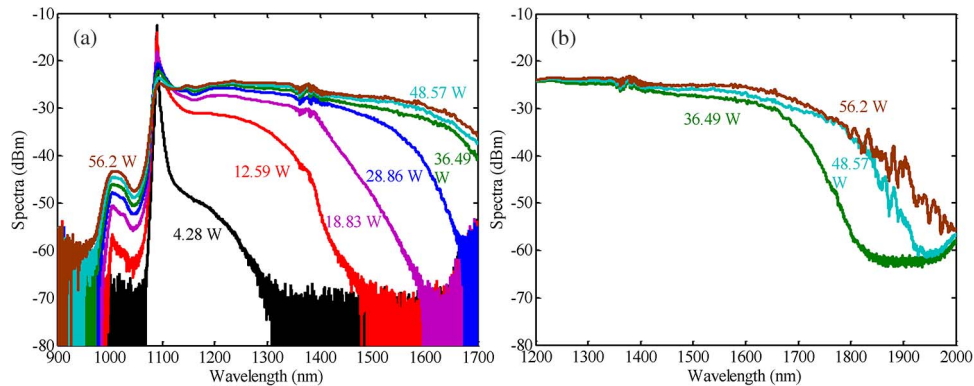


Fig. 7. Output spectra of generated SC pumped by the CW laser. The colored legend presents the power of corresponding spectrum marked by the same color. (a) Spectra below 1700 nm measured by OSA1. (b) Spectra measured by OSA2.

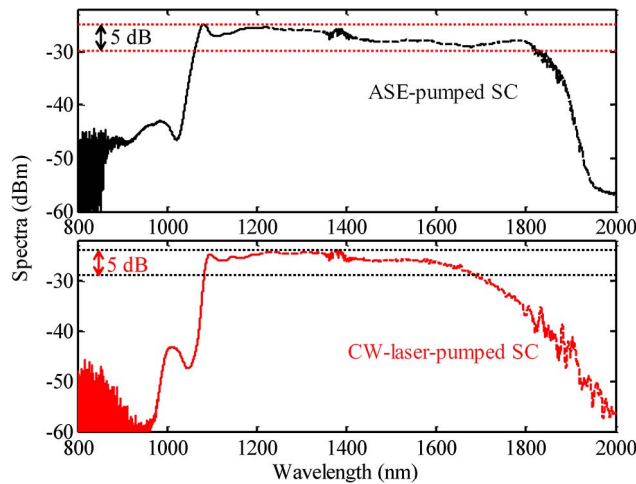


Fig. 8. Spectra of 49.5 W ASE-pumped SC and 56.2 W CW-laser-pumped SC. The spectra presented by full lines are measured by OSA1 (800–1200 nm), and the spectra presented by dashed lines are measured by OSA2 (1200–2000 nm).

from 1082 nm to 1687 nm while the ASE-pumped SC is 49.5 W with 5-dB spectral width 760 nm from 1062 nm to 1822 nm.

4. Conclusion

In this paper, we have experimentally demonstrated a high-power ultra-flat near-infrared SC generation using an incoherent continuous ASE source pumping a section of PCF. A 90.9 W ASE with 3-dB spectrum from 1049 nm to 1072 nm is emitted from a 10- μm -core fiber and then this ASE light is used to pump a 100-m-long PCF. The ASE source is not modulated into bursts to maintain the advantages of CW-pumped SC. Finally, a 49.5 W near-infrared SC generated with 5-dB spectral bandwidth is 760 nm, covering from 1062 nm to 1822 nm. To the best of our knowledge, this is the highest power and flattest spectrum of reported SC sources pumped by ASE sources. In order to make a comparison, this same PCF is pumped by a 122 W CW laser at 1090 nm and a 56.2 W SC is generated with 5-dB spectral width 605 nm from 1082 nm to 1687 nm. The spectral width and flatness of CW-laser-pumped SC are worse than that of ASE-pumped SC. The incoherence of ASE source demonstrates phase and intensity fluctuations, and thus the solitons induced by MI have random bandwidths and durations. Consequently, the

red-shift spectra due to SSFS are distinct from each other, and the averaged spectrum of SC will be smoother than that of SC generated by coherent CW laser. Additionally, the random solitons can strengthen the soliton collisions, which can extend the spectrum to longer wavelength further. Conclusively, using incoherent ASE source as the pump, the conversion efficiency to SC is higher and the spectrum is broader and flatter.

Acknowledgement

The authors would like to thank H. Zhang for help with the construction of the continuous 1090 nm laser.

References

- [1] J. M. Dudley, G. Genty, and S. Coen, "Supercontinuum generation in photonic crystal fiber," *Rev. Mod. Phys.*, vol. 78, no. 4, pp. 1135–1184, Oct. 2006.
- [2] G. Genty, S. Coen, and J. M. Dudley, "Fiber supercontinuum sources (Invited)," *J. Opt. Soc. Amer. B, Opt. Phys.*, vol. 24, no. 8, pp. 1771–1785, Aug. 2007.
- [3] G. P. Agrawal, *Nonlinear Fiber Optics*, 5th ed. Oxford, U.K.: Academic, 2013.
- [4] P. Yan *et al.*, "Polarization dependent visible supercontinuum generation in the nanoweb fiber," *Opt. Express*, vol. 19, no. 6, pp. 4985–4990, Mar. 2011.
- [5] P. Yan *et al.*, "Numerical simulation on the coherent time-critical 2–5 μm supercontinuum generation in an As_2S_3 microstructured optical fiber with all-normal flat-top dispersion profile," *Optics Commun.*, vol. 293, pp. 133–138, Apr. 2013.
- [6] B. A. Cumberland, J. C. Travers, S. V. Popov, and J. R. Taylor, "Toward visible cw-pumped supercontinua," *Opt. Lett.*, vol. 33, no. 18, pp. 2122–2124, Sep. 2008.
- [7] C. Y. Guo *et al.*, "A low-cost CW-pumped supercontinuum source," *Laser Phys.*, vol. 23, no. 5, Apr. 2013, Art. ID. 055403.
- [8] B. H. Chapman, S. V. Popov, and R. Taylor, "Continuous wave supercontinuum generation through pumping in the normal dispersion region for spectral flatness," *IEEE Photon. Technol. Lett.*, vol. 24, no. 15, pp. 1325–1327, Aug. 2012.
- [9] B. H. Chapman, J. C. Travers, S. V. Popov, A. Mussot, and A. Kudlinski, "Long wavelength extension of CW-pumped supercontinuum through soliton-dispersive wave interactions," *Opt. Exp.*, vol. 18, no. 24, pp. 24 729–24 734, Nov. 2010.
- [10] A. Kudlinski, G. Bouwmans, M. Douay, M. Taki, and A. Mussot, "Dispersion-engineered photonic crystal fibers for CW-pumped supercontinuum sources," *J. Lightw. Technol.*, vol. 27, no. 11, pp. 1556–1564, Jun. 2009.
- [11] J. C. Travers, A. B. Rulkov, B. A. Cumberland, S. V. Popov, and J. R. Taylor, "Visible supercontinuum generation in photonic crystal fibers with a 400 W continuous wave fiber laser," *Opt. Exp.*, vol. 16, no. 19, pp. 14 435–14 447, Sep. 2008.
- [12] B. A. Cumberland, J. C. Travers, S. V. Popov, and J. R. Taylor, "29 W high power CW supercontinuum source," *Opt. Express*, vol. 16, no. 8, pp. 5954–5962, Apr. 2008.
- [13] H. Hu, W. Li, S. Ma, and N. K. Dutta, "Coherence properties of supercontinuum generated in dispersion-tailored lead-silicate microstructured fiber taper," *Fiber Integr. Opt.*, vol. 32, no. 3, pp. 209–221, May 2013.
- [14] C. De Matos, S. Popov, and J. Taylor, "Temporal and noise characteristics of continuous-wave-pumped continuum generation in holey fibers around 1300 nm," *Appl. Phys. Lett.*, vol. 85, no. 14, pp. 2706–2708, Oct. 2004.
- [15] F. Vanholsbeeck, S. Martin-Lopez, M. González-Herráez, and S. Coen, "The role of pump incoherence in continuous-wave supercontinuum generation," *Opt. Exp.*, vol. 13, no. 17, pp. 6615–6625, Aug. 2005.
- [16] J. H. Lee, Y.-G. Han, and S. Lee, "Experimental study on seed light source coherence dependence of continuous-wave supercontinuum performance," *Opt. Exp.*, vol. 14, no. 8, pp. 3443–3452, Apr. 2006.
- [17] S. Martin-Lopez *et al.*, "Experimental investigation of the effect of pump incoherence on nonlinear pump spectral broadening and continuous-wave supercontinuum generation," *Opt. Lett.*, vol. 31, no. 23, pp. 3477–3479, Dec. 2006.
- [18] E. J. R. Kelleher, "Pump wave coherence, modulation instability and their effect on continuous-wave supercontinua," *Opt. Fiber Technol.*, vol. 18, no. 5, pp. 268–282, Sep. 2012.
- [19] E. J. R. Kelleher, J. C. Travers, S. V. Popov, and J. R. Taylor, "Role of pump coherence in the evolution of continuous-wave supercontinuum generation initiated by modulation instability," *J. Opt. Soc. Amer. B, Opt. Phys.*, vol. 29, no. 3, pp. 502–512, Mar. 2012.
- [20] H. L. Ju, J. J. Eun, and C.-S. Kim, "Incoherent, CW supercontinuum source based on erbium fiber ASE for optical coherence tomography imaging," in *Proc. 14th OECC*, Hong Kong, Jul. 13–17, 2009, pp. 1–2, Paper FD3.
- [21] J.-H. Lee, E.-J. Jung, and C.-S. Kim, "Optical coherence tomography based on a continuous-wave supercontinuum seeded by erbium-doped fiber's amplified spontaneous emission," *J. Opt. Soc. Korea*, vol. 14, no. 1, pp. 49–54, Mar. 2010.
- [22] J. Eun Joo *et al.*, "Spectrally sampled OCT imaging based on 1.7- μm continuous-wave supercontinuum source," *IEEE J. Sel. Top. Quantum Electron.*, vol. 18, no. 3, pp. 1200–1208, May 2012.
- [23] J. H. Lee, C. Kim, Y.-G. Han, and S. B. Lee, "Broadband, high power, erbium fibre ASE-based CW supercontinuum source for spectrum-sliced WDM PON applications," *Electron. Lett.*, vol. 42, no. 9, pp. 549–550, Apr. 2006.
- [24] L. Shenping, A. B. Ruffin, and D. V. Kuksenkov, "Efficient generation of CW supercontinuum in optical fiber pumped by ASE light," presented at the Optical Fiber Commun. Conf., Anaheim, CA, USA, Mar. 5–10, 2006, Paper OWI32.

- [25] Y. Takushima, "High average power, depolarized super-continuum generation using a 1.55- μm ASE noise source," *Opt. Exp.*, vol. 13, no. 15, pp. 5871–5877, Jul. 2005.
- [26] W. Chen, D. Shen, T. Zhao, and X. Yang, "High power Er, Yb-doped superfluorescent fiber source with over 16 W output near 1.55 μm ," *Opt. Exp.*, vol. 20, no. 13, pp. 14 542–14 546, Jun. 2012.
- [27] S.-P. Chen, Z.-J. Liu, Y.-G. Li, K.-C. Lu, and S.-H. Zhou, "Resonantly pumped high power flat L-band erbium-doped superfluorescent fiber source," *Opt. Exp.*, vol. 16, no. 1, pp. 207–212, Jan. 2008.
- [28] K. Chow, Y. Takushima, and Y. Mizuno, "High average power super-continuum generation using a 1 μm ASE noise source," presented at the Conf. Lasers Electro-Optics, Long Beach, CA, USA, May 21, 2006, Paper CFK6.
- [29] K. Chow, "High average power super-continuum generation using 1 μm noise burst and highly-nonlinear photonic crystal fibre," *Electron. Lett.*, vol. 48, no. 13, pp. 781–783, Jun. 2012.
- [30] P. Wang, J. K. Sahu, and W. A. Clarkson, "110 W double-ended ytterbium-doped fiber superfluorescent source with $M^2 = 1.6$," *Opt. Lett.*, vol. 31, no. 21, pp. 3116–3118, Nov. 2006.
- [31] P. Wang and W. A. Clarkson, "High-power, single-mode, linearly polarized, ytterbium-doped fiber superfluorescent source," *Opt. Lett.*, vol. 32, no. 17, pp. 2605–2607, Sep. 2007.
- [32] Q. Xiao, P. Yan, Y. Wang, J. Hao, and M. Gong, "High-power all-fiber superfluorescent source with fused angle-polished side-pumping configuration," *Appl. Opt.*, vol. 50, no. 8, pp. 1164–1169, Mar. 2011.
- [33] X. Zhou, Z. Chen, H. Chen, J. Li, and J. Hou, "Mode field adaptation between single-mode fiber and large mode area fiber by thermally expanded core technique," *Opt. Laser Technol.*, vol. 47, pp. 72–75, Apr. 2013.
- [34] J. M. Dudley and J. R. Taylor, *Supercontinuum Generation in Optical Fibers*. New York, NY, USA: Cambridge Univ. Press, 2010.
- [35] X. Wang *et al.*, "Raman fiber laser-pumped high-power, efficient Ho-doped fiber laser," *J. Opt. Soc. Amer. B, Opt. Phys.*, vol. 31, no. 10, pp. 2476–2479, Oct. 2014.